IEEE Access
Multidisciplinary ⋮ Rapid Review ⋮ Open Access Journal

Received September 1, 2020, accepted September 20, 2020, date of publication September 23, 2020,
date of current version October 6, 2020.

Digital Object Identifier 10.1109/ACCESS.2020.3026049

Demand Response and Dynamic Line Ratings for Optimum Power Network Reliability and Ageing

WEI CHIEH KHOO[1], JIASHEN TEH[1], (Member, IEEE), AND CHING-MING LAI[2], (Senior Member, IEEE)

[1]School of Electrical and Electronic Engineering, Universiti Sains Malaysia (USM), Nibong Tebal 14300, Malaysia
[2]Department of Electrical Engineering, National Chung Hsing University (NCHU), Taichung 402, Taiwan

Corresponding authors: Jiashen Teh (jiashenteh@usm.my) and Ching-Ming Lai (pecmlai@gmail.com)

This work was supported by the Ministry of Education Malaysia Fundamental Research Grant Scheme (FRGS) under Grant 203/PELECT/6071442.

ABSTRACT This study proposes a methodology to optimise the use of average demand loss of each load bus to enhance line ratings and modify load curves, by minimising demand loss and network ageing due to elevated conductor temperatures. The considered lines are connected to load buses, operated with dynamic line rating technology and have actual conductor physical properties. The simulation of line failures considers line loadings, whose values are based on utilizations of the average demand loss of load buses where the lines are connected, and the remaining service life of the conductor. Demand response in the form of peak-shaving and valley-filling is used to modify load demand curves, with the allowable peak load reduced based on utilizations of the remaining average demand loss. The average demand loss values are determined in the preliminary screening module of the proposed method. Various trade-offs between ageing and reliability of the network are solved based on the two-objective non-sorting genetic algorithm and fuzzy decision-making method in the execution module of the proposed method. Results have shown that the proposed method is cost-effective in that it strategically increase line ageing slightly to enhance system reliability, by as much as 71.9%, based on the equal emphasis of network ageing and reliability, when compared with the scenario that only prioritizes the protection of network ageing. Line ageing is also 68.2% lower on average across the entire spectrum of rating exceedance (1% to 25%) compared to the scenario that only prioritizes enhancement of network reliability.

INDEX TERMS Demand response, dynamic line rating, resilience, reliability, optimisation, ageing, overhead lines, flexibility, Monte Carlo.

I. INTRODUCTION

Power networks are committed to provide electricity in a secure, reliable and economical way. Evolving market regulations and pressures to integrate additional renewable energies into power networks will congest power networks further and increase the risk of operations. To be better prepared for these scenarios, economies need new and flexible network-enhancement strategies that improve network power transfer capability while deferring or avoiding major asset investments.

One approach is by contracting customers to reduce a certain amount of demand, which will either be reimbursed or used at other times based on various demand response (DR) programs [1]–[4]. An alternative is by enhancing the transmission overhead line (OHL) rating based on the thermal behaviour of OHL [5], which forms two variants of flexible thermal rating. The first is the dynamic line rating (DLR) system, which utilises data of OHL ambient conditions to determine line ratings in real time [6]. Research has shown that the DLR method is able to improve line rating by 10%–30% with 50% being possible in windy areas [7]–[9]. The second is probabilistic thermal rating (PTR) method, which fixes a predefined risk of overheating the conductor based on historical line ratings. By adjusting the desirable risk level, the continuous, long-term and short-term thermal ratings are determined, of which the latter two are used during network post-fault condition as contingency measures [10]. Although no extra cost is involved in implementing the PTR method, it increases the risk of line ageing due to the probability of elevating the

The associate editor coordinating the review of this manuscript and approving it for publication was Guangya Yang.

conductor temperature above its maximum design temperature. Moreover, the PTR method may undermine the actual capacity of the OHL when the ambient condition is conducive to higher line ratings. By contrast, the DLR method has none of these drawbacks and can always achieve maximum line ratings based on the selected conductor temperature. However, the risk of determining the optimum conductor temperature, which affects line ageing, has never been quantified by network operators. Thus, informed decision on the acceptable conductor temperature and DR values cannot be made.

Some studies have attempted to model the effects of OHL ageing on network reliability. In [11], [12] the ageing effect of OHL line due to the DLR method and its parametric uncertainty towards the probability of line failure is considered. In [13], [14] the ageing effects of OHL operated with the PTR method towards the reliability of the network is considered. In [15], [16], cable ageing within a distribution network is modelled and the cables are ranked according to ageing criticality to determine replacement priority for achieving optimum network reliability. These studies present various ageing models for OHL and cables and demonstrate the effects of ageing on the reliability of networks. However, no solution has been suggested to address the ageing effects and, as a result, the compromise between reliability benefits and possible asset management plans is never considered. From the perspective of DR, the program has been used and studied previously during normal and contingency operation of the networks [17]–[19]. More importantly, the initiatives of emergency demand response program is investigated and certain values of contractual power and duration (CPD) are determined and used to improve network reliability. Results from these studies indicate that the efficient utilisation of CPD is able to maintain reliability levels during contingencies and subsequently reduce overall network cost.

Based on the preceding review and to the best of our knowledge, no work has considered network ageing, reliability and the optimum usage of CPD values for enhancing network reliability. Thus, this study proposes an optimisation framework that integrates DLR and DR valuation into a single model that is employable by system operators as a flexible strategy. The novelty lies in the optimum utilisation of the CPD to improve network reliability without causing excessive ageing. The proposed framework is also customisable, providing system operators the flexibility to determine various priority levels of reliability and ageing depending on evolving requirements and scenarios. Consequently, the proposed framework enhances existing asset management practices and improves the decision-making process.

II. METHODOLOGY

The proposed reliability evaluation framework utilises network, OHL and weather data to determine CPD values of each load bus in the preliminary screening module. In turn, all these data and the settings of the DR aggregator, which describe the participation availability and duration of each load bus, are used in the execution module where

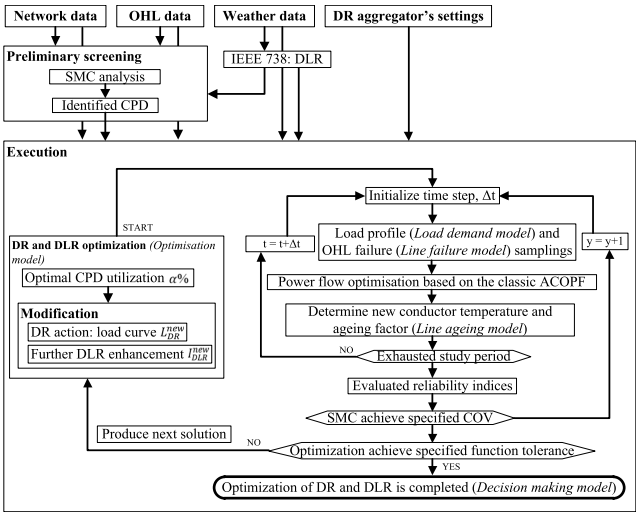

FIGURE 1. Flowchart of proposed DR and DLR synergy for optimum network reliability and ageing.

the utilisation of the CPD is optimised to achieve minimum demand loss and network ageing, as shown in Fig. 1.

The *network data* used include bus voltage limits, generator power constraints, hourly chronological load demand pattern, network topology which describes the arrangement of all power components, i.e. lines, cables, transformers and reliability data of each component based on operator's historical record. The *OHL data* include various design aspects such as diameter, resistance at low and high temperatures, number of strands, rated strength and conductor type, the details of which are available in [20]. The *weather data* include all parameter inputs of IEEE 738 [5] such as wind speed, wind angle, ambient temperature and solar radiation angle and intensity, which are considered to surround the OHLs of the investigated network and are crucial in determining their DLRs and ageing risk.

A. PRELIMINARY SCREENING MODULE

In the preliminary screening module, the classic sequential Monte Carlo (SMC) simulation [21] is performed. At each time step, Δt, the up–down statuses of all power system components, excluding the generators, are simulated. The reason is that the reliability of generators are generally much lower than the OHLs and are excluded to avoid their failures from masking the effect of load loss due to transmission network congestion [22]. The OHLs also operate at their ageing temperature, which is the maximum conductor temperature before ageing occurs, determined based on the IEEE 738 standard [5]s. At each Δt of the SMC, the standard alternative-current optimal power flow (ACOPF) is executed [23], i.e. load shedding is minimised and generation re-dispatched is prioritised when corrective actions are required. During the SMC, the expected energy not supplied (EENS) at each load bus is tracked and the simulation is performed until convergence of the system EENS is achieved. In addition, the expected duration of load curtailment (EDLC)

and expected frequency of load curtailment (EFLC) at each load bus are also recorded. Based on the indices, the contractual power, CP_b, and duration, CD_b, of each load bus b, are obtained as follows:

$$CP_b = \frac{\text{EENS}_b \text{ MWh/y}}{\text{EDLC}_b \text{ h/y}}, \tag{1}$$

$$CD_b = \frac{\text{EDLC}_b \text{ h/y}}{\text{EFLC}_b \text{ occ/y}}, \tag{2}$$

where CP_b and CD_b are passed into the execution module in which negotiation is performed to utilise their values for the optimum proportions of DR action and DLR uprating to minimise system EENS and ageing.

B. EXECUTION MODULE

The execution module considers a new rating limit of the OHLs in addition to the DLRs determined in the preliminary module and modified load due to the DR action. Thus, the uprated DLRs, I_{DLR}^{new}, and new load demand pattern, L_{DR}^{new}, that are the result of the optimum utilisation of the CPD values are considered in the ACOPF of this module.

Fig. 1 shows that the module at each Δt begins by checking for contingency, i.e. load loss and failures of OHLs. Then, based on the optimal usage (see section III.D) of the CPD values, I_{DLR}^{new} and L_{DR}^{new} are determined and ACOPF is executed. Then, every OHL considered for DLR uprating are checked for increment in its conductor temperature, T_c, beyond its ageing temperature, T_{age}, which is 95 °C as the aluminium conductor steel reinforce (ACSR) type conductor is considered for all OHLs [13]. The obtained T_c is used to determine the ageing factor of the OHL (see section III.C). Note that at each Δt, when the CPD values are utilised, the load pattern of each load bus is modified with $\alpha\%$ of the CPD value via the DR action. However, only the OHLs that are at that time sending power to the load bus will have their DLRs uprated by the remaining unused CPD values, i.e. $\beta = (1-\alpha)\%$. The process is performed until the final t hour and is repeated for as many times as required until the EENS coefficient of variation is less than 5%. In every iteration of the SMC, operating temperatures and the remaining service life of the OHLs are considered when their statuses are simulated (see section III.B). Upon convergence of the simulation, the network EENS and expected total network ageing (ETNA) are computed, which also serve as the two objectives used by the optimisation algorithm to check for a specified function tolerance as the stopping criteria. As long as the tolerance is not met, the next value of α is selected and the process is repeated.

The graphical description of various optimisation scenarios encountered in the execution model is shown in Fig. 2. In the first scenario, no flexibility is available in the network and the ENS encountered is the largest (A1). Conductor temperatures are not elevated and peak loads are not avoided. In the second scenario, the CPD values are used entirely to minimise only the network ageing, i.e. ETNA. As a result, OHL conductor temperatures are maintained at 95 °C as in

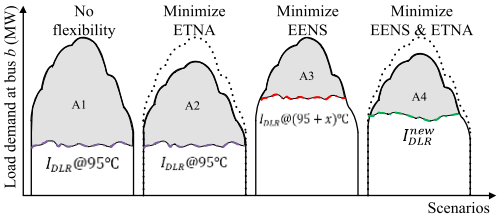

FIGURE 2. Example of proposed optimisation for improved implementation of DR and DLR.

the previous scenario and the entire CPD value is used to modify load demand usage through the DR action, which resulted in the smaller ENS as shown by A2. Although demand loss is reduced, it is never optimised and could be reduced further if conductor temperatures are strategically raised. In contrast to the second scenario, the third scenario dedicates the entire CPD values to minimising load loss instead, i.e. EENS. Owing to this condition, conductor ageing is never considered and line ratings are raised to an arbitrary high value to enhance the power-transfer capability of the network, thereby resulting in smaller ENS shown by A3 compared with A2. Despite the larger reduction of demand loss in this scenario than in A2, excessive conductor ageing is encountered due to extreme elevated conducted temperature. This condition is detrimental to asset management planning and incurs overall higher cost due to more frequent line replacements and repairs. In the final scenario, the utilisation of CPD values are optimised (α and β) to reduce the EENS and ETNA. The conductor temperature of the final scenario is raised to a level between the previous two scenarios at the expense of higher load loss, i.e. A3 $\leq$ A4 $\leq$ A2. This condition enhances the flexibility of the network operators to achieve the most balanced condition between demand loss and network ageing. Due to the conflicting EENS and ETNA, the proposed optimisation framework is an effective way to solve this problem.

III. MODELLING DETAILS

A. LOAD DEMAND MODEL

The proposed methodology is based on the reliability of the DR aggregator in utilising the contractual power, CP_b, during each contingency at each load bus. Based on the uniform random availability, u, of the aggregator, between 0 and 1, the available contractual power, P_b^{CP}, at each simulation time step, Δt, is as follows:

$$P_b^{CP}(t) = u(t) \times CP_b. \tag{3}$$

The load demand curve is modified by the DR action based on $P_b^{CP}(t)$ of each load bus. Then, the modification is performed by reducing the original load demand level that is more than $l\%$ of the peak load, L_b^{peak}, by a fraction, α_b, ranging between 0 and 1, of $P_b^{CP}(t)$, such as:

$$L_{DR}^{red}(t) = L_b(t) - \alpha_b P_b^{CP}(t) \quad \forall t \in \Omega_\psi, \tag{4}$$

where $L_{DR}^{red}(t)$ is the new load demand for all the time when load reduction occurs, Ω_ψ is the set of times when $L_b(t) > l\% \times L_b^{peak}$, and $L_b(t)$ is the original load demand level. The load removed is restored immediately in the next hour by dividing them equally throughout the contractual duration, CD_b, of the bus as follows:

$$L_{DR}^{res}(t) = L_b(t) + \frac{L_b^{red}}{CD_b} \leq l\% \times L_b^{peak} \quad \forall t \in \Omega_\omega, \quad (5)$$

where $L_{DR}^{res}(t)$ is the new load demand for all the time when load restoration occurs, and Ω_ω is the set of times when $L_b(t) < k\% \times L_b^{peak}$ such that $k < l$ to ensure no creation of new peaks after restorations.

B. LINE FAILURE MODEL

Conductor temperature, T_c, and their remaining service life are considered when determining failure rates of lines. The model suitable for relating the OHLs' life with its thermal stress is the Arrhenius model [24], such as the following:

$$L = \mathrm{A}\exp\left(\frac{\mathrm{B}}{T_c + 273}\right), \quad (6)$$

where L is the average life measure of the OHL, and A and B are empirical constants derived from historical loading data [11].

To utilise the Arrhenius model for simulating random line statuses, it needs to be fitted into a suitable probability distribution function (PDF) so that random sampling can be conducted. Moreover, the chosen distribution should have only one life measure, and ultimately, its parameters can capture increasing failure rate in response to higher line loading and useful lifespan. The Weibull distribution shown in (7) fits both of the criteria and has been used previously in the modelling of power transformer [25] and cable [15] failure.

$$F(t) = 1 - \exp\left[-\left(\frac{t}{s}\right)^{\tau}\right], \quad (7)$$

where s is the scale parameter equivalent to L given by (6) and τ is the shape parameter that describes the slope of the Weibull distribution, i.e. the rate of change of the failure probability as time progresses.

Based on polynomial approximation [26] and conditional probability theory [27], the Weibull probability of failure, U, is as follows:

$$U = \frac{1}{\mathbb{N}}\sum_{n=1}^{K} P_n UD_n, \quad (8)$$

where $\mathbb{N}$ is the usefulness duration after the survival period, T, of the OHLs so far; k is the total number of subintervals of $\mathbb{N}$; P_n is the probability of OHL failure considering its remaining service years and loading during subinterval n and the duration, Δl, of each subinterval, as shown in (8a); UD_n is the average duration of P_n, as shown in (8b).

$$P_n = \frac{\exp - \left(\frac{T+(n-1)\Delta l}{s}\right)^{\tau} - \exp\left(-\left(\frac{T+n\Delta l}{s}\right)^{\tau}\right)}{\exp - \left(\frac{T}{s}\right)^{\tau}}, \quad (8a)$$

$$UD_n = \mathbb{N} - (2n-1)\frac{\Delta l}{2}. \quad (8b)$$

The calculated unavailability, U, and a fixed value of repair rate, μ, is used to finally derive the lifespan-and-loading dependent failure rate, λ_L, of the OHLs as in (9). The repair rate is considered constant and known by the utilities as the pace at which repairs are done; this rate is normally controllable depending on allocated priorities and resources.

$$\lambda_L = \frac{\mu U}{1 - U}. \quad (9)$$

C. LINE AGEING MODEL

Accelerated conductor ageing occurs when OHLs operate at temperatures beyond the ageing temperature, T_{age}. This phenomenon is known as "elevated temperature creep" under the IEEE 1283 standard [28]. For the ACSR conductor, this creep, ε_c, is calculated as follows:

$$\varepsilon_c = 0.24\,(\%RS)^{1.3}\,T_c^{1.4}\,t^{0.16}, \quad (10)$$

where $\%RS$ is the percentage remaining strength of the ACSR and t is the number of hours operating at T_c.

The $\%RS$ is determined as follows [29]:

$$RS = RS_{al}\left(\frac{STR_{al}}{STR_T}\right) + 109\left(\frac{STR_{st}}{STR_T}\right), \quad (11)$$

such that

$$RS_{al} = \begin{cases} \gamma t^{\rho} & if\ \alpha < 100 \\ 100 t^{\rho} & otherwise, \end{cases} \quad (11a)$$

$$STR_{al} = \pi \eta_{al} \bar{S}_{al} d_{al} k_{al}/4, \quad (11b)$$

$$STR_{st} = \pi \eta_{st} S_{st}^{1\%} d_{st} k_{st}/4, \quad (11c)$$

where in (11), RS_{al} is the remaining strength of the ACSR's aluminium strand; STR_{al} and STR_{st} are the strength of the ACSR's aluminum and steel strands, respectively; and $STR_T = STR_{al} + STR_{st}$ is the total strength of the ACSR. In (11a), $\gamma = 134 - 0.24T_c$ and $\rho = (0.241 - 0.00254T_c)/d_{al}$, where d_{al} is the diameter of the aluminium strand. The remaining variables in (11b) and (11c), such as η_{al} and η_{st}, are the number of aluminium and steel strands; d_{st} is the diameter of the steel strand; $\bar{S}_{al}$ is the average breaking stress of aluminium; $S_{st}^{1\%}$ is average breaking stress of the steel core at 1% extension; and k_{al} and k_{st} are the reduction factors of aluminium and steel, respectively. All the variables mentioned are found in [20], and only their SI units are used in this study.

As ageing of ACSR occurs when $T_c > T_{age} = 95\,^{\circ}\mathrm{C}$, various ε_c values at different T_c are converted to the equivalent ageing at $T_c = 100^{\circ}\mathrm{C}$ to obtain comparable ageing among all conductors, as in the following:

$$t_{100} = \left(\frac{0.24\left(\%RS_{T_c}\right)^{1.3} T_c^{1.4} t_{T_c}^{0.16}}{0.24\left(\%RS_{T_c}\right)^{1.3} (100)^{1.4}}\right)^{6.25} = \left(\frac{\epsilon_{T_c}}{\epsilon_{100}}\right)^{6.25} \quad (12)$$

Considering all distinct ageing events, N_{age}, of all OHLs, N_{OHL}, for all the simulated years, N_y, the ETNA index as shown in (13) is determined. This index quantifies the risk of network ageing against the utilisation of the CPD value for additional network flexibility as follows:

$$ETNA = \frac{1}{y}\sum_{y=1}^{N_y}\sum_{j=1}^{N_{OHL}}\sum_{i=1}^{N_{age}}\left(\frac{\epsilon_{T_c}}{\epsilon_{100}}\right)^{6.25}\frac{h}{y}. \tag{13}$$

D. OPTIMISATION MODEL

The $EENS_b$ and $ETNA_b$ of load busses are inversely related indices. If ratings of OHLs are increased, then additional power flows are permitted, which lead to further ageing but lower load loss. Conversely, although reducing OHL ratings reduces ageing, it leads to greater load loss due to power flow restrictions. Thus, the two indices is more suitably solved as two- rather than single-objective optimisation during each Δt as in the following:

$$\min_b \begin{bmatrix} f_1(t) \\ f_2(t) \end{bmatrix} = \min \begin{bmatrix} \text{EENS}_b(t, \alpha_b) \\ \text{ETNA}_b(t, \beta_b = 1 - \alpha_b) \end{bmatrix}. \tag{14}$$

Equation (14) shows that at the Δt when contingency occurs, the optimal fraction pair, (α_b, β_b), of each load bus of the available contractual power, P_b^{CP}, is approximated to minimise load loss and ageing of the lines that deliver power to the load bus, which their respective sums provide the $EENS_b$ and $ETNA_b$ upon the convergence of the SMC. The β_b fraction is used to uprate DLRs to I_{DLR}^{new}. When $\beta_b \neq 1$, various levels of OHL ageing are considered at the expense of higher demand loss, i.e. $EENS_b$. On the other hand, when $\beta_b = 1$, the ageing of OHL is neglected and the entire P_b^{CP} is used to reduce $EENS_b$ only. As the reduction of demand loss and uprating of DLRs are based on the usage of P_b^{CP}, the relationship $\alpha_b + \beta_b = 1$ always holds. The following are details of the two objectives of the proposed optimisation model.

Objective 1: To minimise the EENS of the grid based on the proportion of the contractual power utilised as follows:

$$\begin{aligned} \min f_1(t) &= \min\left[\text{EENS}(t, \alpha)\right] \\ &= \min\left[\sum_{b=1}^{N_b} P_b^{loss}\left(\alpha_b P_b^{CP}(t)\right)\right], \end{aligned} \tag{15}$$

where P_b^{loss} is the curtailment of load bus b determined during ACOPF by considering the uprated DLR of OHLs, in which α_b controls various levels of the uprating. N_b is the number of load bus.

Objective 2: To minimise the grid's ETNA based on the remaining proportion, i.e. $\beta = 1-\alpha$, of the contractual power utilised. At each load bus, β_b is used only on lines that are feeding power to the load bus itself instead of all the lines that are connected to the load bus. The reason is that any line with a receiving end that is not connected to the load bus will not affect the demand loss of the load bus, and subsequently, their ageing is affected by other load busses instead. The value of β_b is also divided equally among the feeding lines and the divided fraction is used to uprate their DLRs proportionately. The following is the second objective function:

$$\begin{aligned} \min f_2(t) &= \min\left[\text{ETNA}(t, \beta_b)\right] \\ &= \min\left\{\text{ETNA}\left[\Delta I_{DLR}(t, \beta_b)\right]\right\}, \end{aligned} \tag{16}$$

where (16) shows that the ETNA index is calculated after considering line rating increment, $\Delta I_{DLR}(t, \beta_b)$, on all participating OHLs. The index quantifies the network's additional allowable power flows such that:

$$\begin{aligned} \Delta I_{DLR} &= \sum_{b=1}^{N_b}\sum_{j=1}^{N_{jb}} \Delta I_{DLR,jb} = I_{DLR,jb}^{new} - I_{DLR,jb} \\ &= \beta_{jb} P_b^{CP}, \end{aligned} \tag{17}$$

where subscript jb refers to the feeding line j of bus b, N_{jb} is the total number of feeding lines, $\Delta I_{DLR,jb}$ is the line rating increment of the feeding lines, $I_{DLR,jb}$ is the original DLR of the feeding lines before uprating, and β_{jb} is the equal division of β_b among all the feedings lines of loadbus b. For example, if bus 3 is connected to 3 feeding lines, then $\beta_3 = \beta_{13} + \beta_{23} + \beta_{33}$. (17) shows that if the DR aggregator of bus b is not available, i.e., $u(t) = 0$, which leads to $P_b^{CP} = 0$, then the ageing minimisation of feeding lines j cannot be enforced.

The solution to $ETNA(t, \beta)$ in (16) is given by (12) and (13) but they require the equivalent T_c of I_{DLR}^{new} to be determined. To perform this function, we refer to the IEEE 738 standard [5] as shown in the following:

$$\begin{aligned} &Q_j(I, R(T_c), T_c) + Q_s(\theta) - Q_r(T_c, T_a) \\ &\qquad - Q_c(T_c, T_a, V_w, \phi) = 0, \end{aligned} \tag{18}$$

where (18) is the heat balance (HB) equation describing heat exchanges of OHLs due to its environmental conditions. Q_j and Q_s are the joule and solar heat gains due to current flow I, which is either I_{DLR}^{new} or I_{DLR}, conductor resistance, $R(T_c)$, due to its temperature T_c and solar radiation intensity, θ. Q_r and Q_c are the radiated and convection heat loss due to T_c, ambient temperature T_a, wind velocity V_w and wind angle ϕ. Owing to the non-linear state of (18) and with the knowledge of I and all the remaining variables being the same, the equation is applied backward to determine T_c that satisfies the HB equation. Starting at $T_c = T_a$ and at each iteration, T_c is increased by 0.5 °C, and (18) is recalculated. This back-calculation process is terminated when the successive HB error is less than 1%. The illustration of this process is shown in Fig. 3.

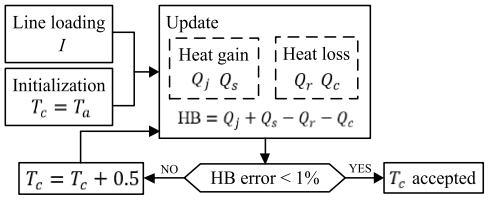

FIGURE 3. Back-calculation process of IEEE 738 standard.

During the optimisation, traditional ACOPF network constraints [30], i.e. rating limits, voltage limits, generation limits

and others are observed. Moreover, the following are also observed:

$$0 \leq \beta_b \leq \beta_b^{max} \leq 1, \tag{19}$$

$$\alpha_b + \beta_b = 1 \quad \forall b \in \Omega_b, \tag{20}$$

$$\Delta I_{DLR,jb} = \beta_{jb} P_b^{CP} \leq I_{DLR,jb} \left(P_b^{CP} - 1 \right), \tag{21}$$

where (19) gives utilities the flexibility to assign the maximum fraction value β_b^{max}, so that I_{DLR}^{new} may be limited depending on the present age of connected lines, policy to extend their operational life, acceptable ageing risk of the utilities and the replacement and repair costs of the lines. For example, higher β_b^{max} can be assigned to newer lines because they can afford higher ageing risk than older lines, or at the more congested network area to free up power flow and reduce demand loss. (20) ensures that the sum of the assigned fractions at all load busses will never exceed unity, and Ω_b is the set of all load busses. The constraint in (21) ensures that the uprating of DLR is always within the available contractual power, P_b^{CP}, dedicated to rating enhancement.

Owing to the inverse relationship of the EENS and ETNA, the non-linear and non-convex nature of the optimisation and the Pareto optimality factor, i.e. none of the indices can be improved without degrading the value of the other, they are both solved based on the common operations of the non-sorting genetic algorithm (NSGA) [31], i.e., mutation, crossover and selection, which has been widely used and applied in various power system studies [32], [33]. The following is the description of the NSGA applied in this paper:

1) Initializes a random initial parent population, which consists of 100 random α_b and $\beta_b = 1 - \alpha_b$ vectors. Each vector (individual) has 17 inputs, one for each load bus, and all inputs randomly range between 0 and 1.
2) Creates a sequence of next generation of populations (number remain at 100) from among the parent individuals, by performing the following steps:
   a) Scores the fitness values of each individual based on (14) to (17) and randomly group all individuals into the tournament size of four.
   b) The best performing (lowest EENS or ETNA) individual of each group is selected and passed down unchanged as children in the next generation, in a process called elitism.
   c) The remaining two out-of three individuals of each group are randomly selected for crossovers to produce new individuals (children) of the next generation; random fractions and complement size of the two individuals are exchanged to produce two children. Crossover enables the algorithm to extract the best genes from different individuals and recombine them into potentially superior children.
   d) The remaining final individual of each group has a fraction of its vector entries randomly selected and all entries of this fraction have 0.01 probability of being modified and replaced with a random value between 0 and 1, in a process called mutation. Mutation provides genetic diversity and enables the genetic algorithm to search a broader space, subsequently increasing the likelihood that the algorithm will generate individuals with better fitness values.
3) The NSGA continues to produce the next generation of individuals, until the average relative change of the best fitness function values (EENS and ETNA) over 100 generations are less than or equal to 0.01%, and when the improvement in one objective requires a degradation of another.

E. DECISION-MAKING MODEL

The outcomes of the NSGA is a range of applicable solutions and additional judgment criteria based on preferences, such as the fuzzy decision method, is used to select the final desirable solution. The fuzzy method works by determining the relative distance of each solution to the maximum and minimum values such as in (22), with 0 and 1 indicating the most undesirable and desirable solutions, respectively.

$$\mu_{f_i}(X) = \begin{cases} 0 & f_i(X) = f_i^{max} \\ \dfrac{f_i^{max} - f_i(X)}{f_i^{max} - f_i^{min}} & f_i^{min} \leq f_i(X) \leq f_i^{max} \\ 1 & f_i(X) = f_i^{min}, \end{cases} \tag{22}$$

where $\mu_{f_i}(X)$ is the relative distance of the point X between the maximum f_i^{max} and minimum f_i^{min} solution of objective i, i.e. either EENS or ETNA. Due to the minimisation requirement of this problem, the minimum solution is assigned 1. Then, the final point $x \in X$ is selected according to the following:

$$\min_{x \in X} = \sum_{i=1}^{N_f} \left| \mu_i - \mu_{f_i}(X) \right|^n, \tag{23}$$

where N_f is the number of solutions, which in this case is 2 (EENS and ETNA) and μ_i is the preference level of the solution, and n is an integer between 1 and ∞. A larger value reduces the sensitivity of the final solution toward n.

IV. RESULTS AND DISCUSSIONS

The proposed optimisation is applied to the IEEE 24-bus reliability test network (RTN) [34] with the load and generation level increased by 3.5 pu. The weather conditions are obtained from the British Atmospheric Data Centre [35] in hourly manner from 2016 until 2019 and is overlaid onto the RTN, with one weather location for each transmission corridor. All lines are also equipped with the DLR system. The RTN is divided into 138 kV and 230 kV voltage zones. The *Drake* and *Lapwing* ACSR conductors are used in the lower and higher voltage zones, respectively. Note that T_{age} of these conductors is 95 °C and thus, the conductor temperature below this level will not induce ageing. When

conductor temperatures are allowed to exceed T_{age}, the excess is only limited to an additional 15% of the value. The setting $\beta_b^{max} = 1$ is also applied to all load busses so that all lines have equal criticality ageing factor. The network is considered to have 40 years of remaining service life. The DR scheme is implemented at $l = 80\%$ and $k = 60\%$ of the RTN peak load. Note that transformers and underground cables reliability and ageing aspects are not considered as the focus of this paper is on overhead transmission lines.

The CPD values, CP_b and CD_b, identified in the preliminary screening module are shown in Fig. 4. They values are all matched and used as the basis for executing the optimisation as detailed in the optimisation model. The figure shows no CPD values in load busses 7 and 15 as their EENS indices are zero.

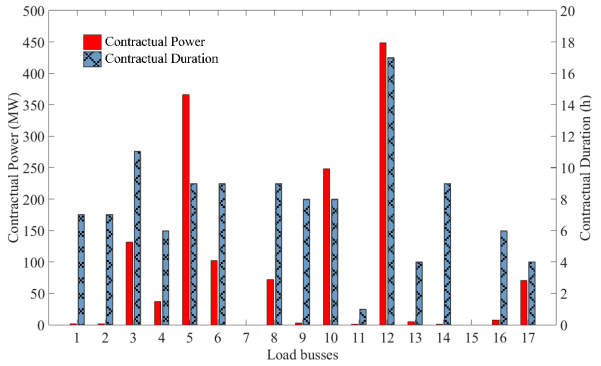

FIGURE 4. CPD values identified in the initialisation module.

A. OPTIMISED UTILISATION OF CPD VALUES

The Pareto solutions of the proposed optimisation are shown in Fig. 5, and the selected optimum α_b and β_b values for every load bus based on the equal preference ($\mu_1 = \mu_2 = 0.5$) of EENS and ETNA are presented in Fig. 6.

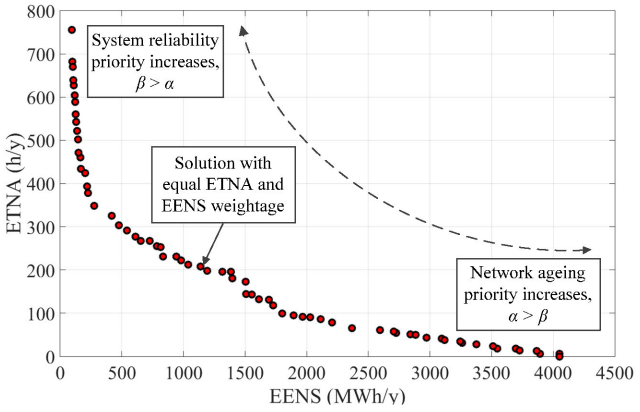

FIGURE 5. Pareto front of proposed optimisation.

The first Pareto solution (left most) in Fig. 5 is obtained when system reliability is most prioritized over network ageing, which is the case where entire CP_b values is used to uprate DLR and line ageing due to excessive loading is less concerned. Under this setting, although the EENS is minimum at approximately 96 MWh/y, the ETNA is at the maximum, which is approximately 755 h/y. On the other hand, the last Pareto solution (right most) is obtained when network ageing is most prioritized instead over system reliability. In this setting, line ageing is avoided entirely (0 h/y) and all CP_b values are utilised for DR action only, resulting in EENS of approximately 4051 MWh/y. This relatively high level of EENS shows that although DR scheme is able to reduce the burden of power generators by levelling peak loads, its benefits towards system reliability is limited by the bottlenecked power transfer capability of the network which inhibit more demand to be served. In general, the Pareto solutions exhibit that the EENS and ETNA are inversely related and the chosen solution based on the equal preference setting in the decision-making model is also highlighted in Fig. 5. This preference setting can be modified based on network conditions and reliability requirement. For example, the network with more old lines cannot afford high ETNA and thus, higher EENS has to be accepted, as shown on the right side of the figure and vice versa.

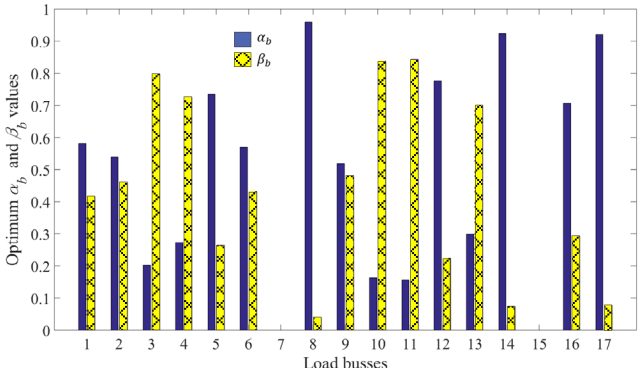

FIGURE 6. Optimum choice of α and β values for each load bus based on equal criterion fuzzy decision-making model.

Fig. 6 shows that busses 3, 4, 10, 11 and 13 utilize most ($\beta_b > 0.5$) of their CP_b values to uprate DLRs of lines connecting to them. The accumulated load at busses 3, 4 and 10 constitute on average 15.7% of the total load in the network and none of them have a local generator. Such condition forces all the load demand to be matched only by power imported from other generators located in remote busses. In addition, theses load busses are connected with at least two feeding lines most of the time, which creates a conducive environment for utilizing a substantial amount of their CP_b values to uprate DLRs of their feeding lines without causing excessive line ageing due to sharing of the uprating burden among the lines. Although load busses 11 and 13 have local generators, they are high capacity generators which have huge surpluses even after matching local demand and the remaining is therefore exported to other busses. In contrast to the earlier mentioned load busses, load busses 11 and 13 are connected with at least two exporting instead of importing

lines most of the time. Due to this, uprating burden can be shared and majority of their CP_b values can safely be used to uprate DLRs. The remaining load busses 1, 2, 5, 6, 9, 12, 14, 16 and 17 dedicate most ($\alpha_b > 0.5$) of their CP_b values to implementing the DR scheme. The main reason is the demand on these load buses are generally small and on average constitute approximately only 4.7% of the total load demand. Therefore, the necessity to uprate DLRs of their connecting lines is lesser and the DR action is significant enough to mitigate most of the EENS on these load busses. Finally, load buses 7 and 15 are left out in the optimization as there are no CPD values on them and therefore nothing to be utilized.

TABLE 1. Summary of reliability indices.

Scenarios	EENS MWh/y	ETNA h/y	EIC M$/y	ETNC k$/y
S1 (No flexibility)	5539	0	45.42	0
S2 ($\alpha = 0, \beta = 1$)	96	755	0.79	204.38
S3 ($\alpha = 1, \beta = 0$)	4051	0	33.20	0
S4 ($\mu_1 = \mu_2 = 0.5$)	1140	208	9.35	56.31

B. RELIABILITY EFFECTS OF OPTIMISATION SCENARIOS

The considered optimisation scenarios in this section are described in Table I and their reliability impacts are compared. S1 is the base case where none of the CPD is utilized for added flexibility as proposed in this study. S2 minimizes system reliability without considering network ageing. In contrast, S3 ignores system reliability and seeks to minimize network ageing only. S4 is our proposed optimization with equal criterion setting in the fuzzy decision making model. In addition to EENS and ETNA, new indices such as the expected interruption cost (EIC) and expected total network cost (ETNC) are also recorded. The EIC is calculated based on the rate $8200/MWh [36], while the ETNC is calculated by considering: (1) total ACSR length of the RTN, which has 766 km and 689 km of Drake and Lapwing ACSR, respectively, (2) manufacturing price of ACSR, which is quoted at approximately $178/km and $195/km for the Drake and Lapwing ACSR, respectively [37], and (3) 1,000 hours of conductor thermal ageing limit of the ACSR [38].

In S1, OHLs are limited to 95 °C and none of the CPD values are utilised to reduce peak demands. Due to this condition, S1 has the highest EENS and subsequently, the highest EIC of 45.42 M$/y. When CPD values are used to add flexibility to the RTN by levelling peak demands in S3, the EENS and EIC drop significantly by 26.9% compared with S1. As no initiative is used to uprate the DLR of the lines, no reported network ageing is reported in S3. By contrast, S2 dedicates all the CPD values to uprate DLR, but peak demands are not shaved. In this scenario, conductor temperatures are raised beyond $T_{age} = 95$ °C to ensure that the generated power has the best avenue to be delivered to every load point. Due to this condition, the EENS is the lowest in S2, but the ETNA suffers by being raised to 755 h/y, which costs approximately 204.38 k$/y, compared with S1 and S3. Instead of reducing only either the EENS or ETNA, S4 minimises both based on the proposed optimisation model. Although the EENS in this scenario is greater than that of S2, its value is still much lower than the EENS of S1 and S3 by approximately 79.4% and 71.9%, respectively. In terms of ETNA, the network ageing of S4 is also lower than that of S2 by approximately 72.5%, a significant 148.07 k$/y saving, which compensates for the 8.56 M$/y increase in EIC value.

C. CONDUCTOR TEMPERATURE EXCEEDANCE EFFECTS

In this section, the exceedance limit of the conductor temperature varies from an additional 1% to 25% of T_{age} with all other remaining settings being the same. Within the range, 9% to 12% is the common practice in the UK [39]. Due to the studied parameter, only S2 and S4 are affected, as shown by the results in Fig. 7. The 15% exceedance value shown in figure denotes the value reported in Table I.

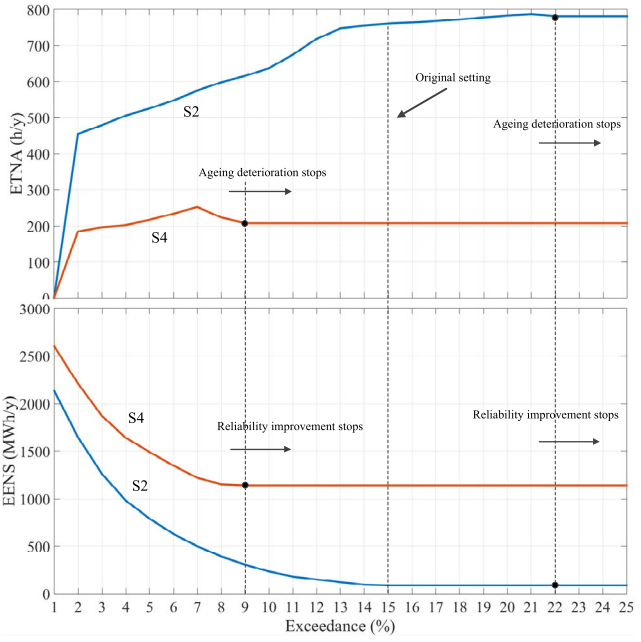

FIGURE 7. Exceedance effects on ETNA and EENS.

The result shows that ETNA in both S2 and S4 increase together with the exceedance percentage, while their EENS are inversely related. Due to S2 ignoring line ageing and prioritizing system reliability only, it has ETNA and EENS that are higher and lower than S4, respectively, across the entire investigated exceedance range. However, both the indices in S4 stops reacting after 9% exceedance, while in S2 the reaction stops much later after 22%. The reason this happens is due to the proportion of the contractual power, CP_b, used to uprate DLRs has been entirely used at these points. Therefore, further increasing the limit of exceedance has no more effects towards the DLRs. Due to the emphasis of S2, it has higher line uprating potential which takes 13% more exceedance

than 9% in S4 in order to completely exhaust the contractual power.

Notice that ETNA drops slightly at 7% and 21% before flatting out in S4 and S2, respectively. Prior to these levels, the rating limit is lower than the amount of CP_b dedicated for line uprating. As a result, the ceiling of line rating limit is always met after uprating, which can only be increased further by increasing exceedance level. However, beyond these points enough line rating limits are unlocked to share the uprating burden to cause ETNA to decrease slightly before levels out when the entire proportion of CP_b has been used for line uprating. The result indicates that S4 induces less ageing than S2 within any particular exceedance level by 68.2% on average. Therefore S4 allows higher line capacity with significant lower ageing risk.

V. CONCLUSION

This study proposes a two-objective optimisation methodology in utilising the CPD values for minimising network demand loss and ageing. The proposed method is applied on every load bus and gives the network operator the flexibility to adjust the ageing level against power-transfer capability by varying the α and β values. Thus, the contribution of the CPD values toward network ageing and reliability is controlled, and informed OHL management strategies can be devised and executed. Results have shown that the proposed method is balanced and more cost-effective when EENS and ETNA are considered together. Our results show that the equal emphasis of EENS and ETNA in S4 bring about 71.9% improvement in system reliability compared to S3 (avoiding line ageing) although line ageing was increased from 0 h/y to 208 h/y. On average, S4 reported 68.2% less ageing than S2 (avoiding load loss) across the entire spectrum of investigated rating exceedance (1% to 25%). In future studies, new and specific OHL health indices can be incorporated into the proposed optimisation framework so that a more robust and customised assessment can be performed. This approach can also be extended to include the effects of weather conditions and hostile operating environments. The limitation of this study is the lacking of a full economic model that associates costs to utilizations of demand loss, OHL ageing, OHL replacement/investment activities, load interruptions, generator operations and carbon emissions levels. Such a model is valuable for adjusting network ageing and reliability risks based on various asset management platforms in terms of economic criteria, further quantifying additional values of the optimization presented in this paper.

REFERENCES

[1] H. Jabir, J. Teh, D. Ishak, and H. Abunima, "Impacts of demand-side management on electrical power systems: A review," *Energies*, vol. 11, no. 5, p. 1050, Apr. 2018.

[2] J. Teh, C. Ooi, Y.-H. Cheng, M. Atiqi Mohd Zainuri, and C.-M. Lai, "Composite reliability evaluation of load demand side management and dynamic thermal rating systems," *Energies*, vol. 11, no. 2, p. 466, Feb. 2018.

[3] H. J. Jabir, J. Teh, D. Ishak, and H. Abunima, "Impact of demand-side management on the reliability of generation systems," *Energies*, vol. 11, no. 8, p. 2155, Aug. 2018.

[4] J. Teh, "Adequacy assessment of wind integrated generating systems incorporating demand response and battery energy storage system," *Energies*, vol. 11, no. 10, p. 2649, Oct. 2018.

[5] *IEEE Standard for Calculating the Current-Temperature of Bare Overhead Conductors*, IEEE Standard 738-2006 (Revision of IEEE Std 738-1993), 2007, pp. 1–59.

[6] J. Teh, C.-M. Lai, N. A. Muhamad, C. A. Ooi, Y.-H. Cheng, M. A. A. Mohd Zainuri, and M. K. Ishak, "Prospects of using the dynamic thermal rating system for reliable electrical networks: A review," *IEEE Access*, vol. 6, pp. 26765–26778, 2018.

[7] J. Teh and I. Cotton, "Reliability impact of dynamic thermal rating system in wind power integrated network," *IEEE Trans. Rel.*, vol. 65, no. 2, pp. 1081–1089, Jun. 2016.

[8] J. Teh and I. Cotton, "Critical span identification model for dynamic thermal rating system placement," *IET Gener., Transmiss. Distrib.*, vol. 9, no. 16, pp. 2644–2652, Dec. 2015.

[9] J. Teh and I. Cotton, "Risk informed design modification of dynamic thermal rating system," *IET Gener., Transmiss. Distrib.*, vol. 9, no. 16, pp. 2697–2704, Dec. 2015.

[10] T. O. Seppa, "A practical approach for increasing the thermal capabilities of transmission lines," *IEEE Trans. Power Del.*, vol. 8, no. 3, pp. 1536–1550, Jul. 1993.

[11] J. Teh, C.-M. Lai, and Y.-H. Cheng, "Impact of the real-time thermal loading on the bulk electric system reliability," *IEEE Trans. Rel.*, vol. 66, no. 4, pp. 1110–1119, Dec. 2017.

[12] J. Teh, "Uncertainty analysis of transmission line End-of-Life failure model for bulk electric system reliability studies," *IEEE Trans. Rel.*, vol. 67, no. 3, pp. 1261–1268, Sep. 2018.

[13] K. Kopsidas, C. Tumelo-Chakonta, and C. Cruzat, "Power network reliability evaluation framework considering OHL electro-thermal design," *IEEE Trans. Power Syst.*, vol. 31, no. 3, pp. 2463–2471, May 2016.

[14] J. Teh and C.-M. Lai, "Risk-based management of transmission lines enhanced with the dynamic thermal rating system," *IEEE Access*, vol. 7, pp. 76562–76572, 2019.

[15] M. Buhari, V. Levi, and S. K. E. Awadallah, "Modelling of ageing distribution cable for replacement planning," *IEEE Trans. Power Syst.*, vol. 31, no. 5, pp. 3996–4004, Sep. 2016.

[16] M. Buhari, V. Levi, and A. Kapetanaki, "Cable replacement considering optimal wind integration and network reconfiguration," *IEEE Trans. Smart Grid*, vol. 9, no. 6, pp. 5752–5763, Nov. 2018.

[17] Y. Zhou, P. Mancarella, and J. Mutale, "Modelling and assessment of the contribution of demand response and electrical energy storage to adequacy of supply," *Sustain. Energy, Grids Netw.*, vol. 3, pp. 12–23, Sep. 2015.

[18] B. Hayes, I. Hernando-Gil, A. Collin, G. Harrison, and S. Djokic, "Optimal power flow for maximizing network benefits from demand-side management," *IEEE Trans. Power Syst.*, vol. 29, no. 4, pp. 1739–1747, Jul. 2014.

[19] M. M. Sahebi, E. A. Duki, M. Kia, A. Soroudi, and M. Ehsan, "Simultanous emergency demand response programming and unit commitment programming in comparison with interruptible load contracts," *IET Generat. Transmiss. Distrib.*, vol. 6, no. 7, pp. 605–611, Jul. 2012.

[20] Southwire Company. *LLC*. Accessed: Sep. 25, 2020. [Online]. Available: http://www.southwire.com/Ordering.htm

[21] R. Billinton and R. N. Allan, *Reliability Evaluation of Power Systems*. New York, NY, USA: Plenum, 1984.

[22] J. Teh and C.-M. Lai, "Reliability impacts of the dynamic thermal rating system on smart grids considering wireless communications," *IEEE Access*, vol. 7, pp. 41625–41635, 2019.

[23] H. Abunima, J. Teh, C.-M. Lai, and H. Jabir, "A systematic review of reliability studies on composite power systems: A coherent taxonomy motivations, open challenges, recommendations, and new research directions," *Energies*, vol. 11, no. 9, p. 2417, Sep. 2018.

[24] H. Hirose and T. Sakumura, "Foundation of mathematical deterioration models for the thermal stress," *IEEE Trans. Dielectrics Electr. Insul.*, vol. 22, no. 1, pp. 482–487, Feb. 2015.

[25] S. K. E. Awadallah, J. V. Milanovic, and P. N. Jarman, "Quantification of uncertainty in End-of-Life failure models of power transformers for transmission systems reliability studies," *IEEE Trans. Power Syst.*, vol. 31, no. 5, pp. 4047–4056, Sep. 2016.

[26] W. Li, "Incorporating aging failures in power system reliability evaluation," *IEEE Trans. Power Syst.*, vol. 17, no. 3, pp. 918–923, Aug. 2002.

[27] R. Billinton and R. N. Allan, *Reliability Evaluation of Engineering systems: Concepts and Techniques*. Harlow, U.K.: Longman Scientific & Technical, 1987.

[28] *IEEE Approved Draft Guide for Determining the Effects of High Temperature Operation on Conductors, Connectors, and Accessories*, IEEE Standard P1283/D8, Apr. 2013, pp. 1–39.
[29] J. Harvey, "Effect of elevated temperature operation on the strength of aluminum conductors," *IEEE Trans. Power App. Syst.*, vol. PAS-91, no. 5, pp. 1769–1772, Sep. 1972.
[30] R. D. Zimmerman, C. E. Murillo-Sanchez, and R. J. Thomas, "MATPOWER: steady-state operations, planning, and analysis tools for power systems research and education," *IEEE Trans. Power Syst.*, vol. 26, no. 1, pp. 12–19, Feb. 2011.
[31] J. Teh, C.-M. Lai, and Y.-H. Cheng, "Improving the penetration of wind power with dynamic thermal rating system, static VAR compensator and multi-objective genetic algorithm," *Energies*, vol. 11, no. 4, p. 815, Apr. 2018.
[32] H.-Y. Su and H.-H. Hong, "A stochastic multi-objective approach to pilot bus selection for secondary voltage regulation," *IEEE Trans. Power Syst.*, vol. 35, no. 4, pp. 3262–3265, Jul. 2020.
[33] A. A. Eshkaftaki, A. Rabiee, A. Kargar, and S. T. Boroujeni, "An applicable method to improve transient and dynamic performance of power system equipped with DFIG-based wind turbines," *IEEE Trans. Power Syst.*, vol. 35, no. 3, pp. 2351–2361, May 2020.
[34] C. Grigg, P. Wong, P. Albrecht, R. Allan, M. Bhavaraju, R. Billinton, Q. Chen, C. Fong, S. Haddad, S. Kuruganty, W. Li, R. Mukerji, D. Patton, N. Rau, D. Reppen, A. Schneider, M. Shahidehpour, and C. Singh, "The IEEE reliability test system-1996. A report prepared by the reliability test system task force of the application of probability methods subcommittee," *IEEE Trans. Power Syst.*, vol. 14, no. 3, pp. 1010–1020, 1999.
[35] *British Atmospheric Data Center (BADC)*. Accessed: Sep. 25, 2020. [Online]. Available: http://badc.nerc.ac.uk/data/ukmo-midas/WPS.html
[36] *Counting the Cost: The Economic and Social Costs of Electricity Shortfalls in the UK*. London, U.K.: Royal Academy of Engineering, Nov. 2014.
[37] *BA52: Bare Aluminum Conductor Price Sheet*. Carrollton, GA, USA: Southwire, 2019.
[38] R. Thrash, A. Nurrah, M. Lancaster, and K. Knuckles, *Overhead Conductor Manual*. Carrollton, GA, USA: Southwire, 2007.
[39] *Electricity Ten Year Statement*. Warwick, U.K.: National Grid Electricity Transmission, 2014.

WEI CHIEH KHOO received the B.Eng. degree in mechanical engineering from Universiti Tenaga Nasional (UNITEN), Selangor, Malaysia, in 2008, and the Master in Business Administrations (M.B.A.) degree from Universiti Sains Malaysia (USM) in 2016, where he is currently pursuing the Ph.D. degree in power and energy field.

JIASHEN TEH (Member, IEEE) received the B.Eng. degree (Hons.) in electrical and electronic engineering from Universiti Tenaga Nasional (UNITEN), Selangor, Malaysia, in 2010, and the Ph.D. degree in electrical and electronic engineering from the University of Manchester, Manchester, U.K., in 2016.

Since 2016, he has been a Senior Lecturer/Assistant Professor with Universiti Sains Malaysia (USM), Penang, Malaysia. In 2018, he was appointed and served as an Adjunct Professor with the Green Energy Electronic Center, National Taipei University of Technology (Taipei Tech), Taipei, Taiwan. Since 2019, he has been an Adjunct Professor with the Intelligent Electric Vehicle and Green Energy Center, National Chung Hsing University (NCHU), Taichung, Taiwan. His research interests include probabilistic modeling of power systems, grid-integration of renewable energy sources, and reliability modeling of smart grid networks.

Dr. Teh is a member of the IEEE Power and Energy Society and the Institution of Engineers Malaysia (IEM). He received the Outstanding Publication Awards from USM in 2017 and 2018. He is also a Regular Invited Reviewer for *International Journal of Electrical Power and Energy Systems*, IEEE Access, IEEE Transactions on Industry Applications, IEEE Transactions on Vehicular Technology, IEEE Transactions on Reliability, IEEE Transactions on Industrial Electronics, and *IET Generation, Transmission and Distribution*. He is a Chartered Engineer (CEng) conferred by the Engineering Council, U.K., and The Institution of Engineering and Technology (IET). He is also a Registered Professional Engineer (P.Eng.) with the Board of Engineers Malaysia (BEM).

CHING-MING LAI (Senior Member, IEEE) received the Ph.D. degree in electrical engineering from National Tsing Hua University, Hsinchu, Taiwan, in 2010.

From 2009 to 2012, he was a Senior Research and Development Engineer with Lite-ON Technology Corporation, Taiwan, where he worked on the high-efficiency and high-power-density power supply. In 2012, he established UPE-Power Technology Company Ltd., Taichung, Taiwan, the company is mainly developing switching power supplies. From 2014 to 2019, he was a Faculty Member with the Department of Vehicle Engineering, National Taipei University of Technology (Taipei Tech). Since 2019, he has been an Associate Professor with the Department of Electrical Engineering, National Chung Hsing University (NCHU), Taiwan, where he is also the Director of the Intelligent Electric Vehicle and Green Energy Center (i-Center). His research interests include electric vehicles (EVs), power electronics, and high-efficiency energy power conditioning systems.

Dr. Lai is an IET Fellow and a Life Member of the Taiwan Power Electronics Association (TaiPEA), the Society of Automotive Engineers Taipei (SAE-Taipei), the Chinese Institute of Electrical Engineering (CIEE), the Chinese Institute of Engineers (CIE), the Taiwan Association of Systems Science and Engineering (TASSE), and the Taiwan Power and Energy Engineer Association. He is also a member of the IEEE Power Electronics, the IEEE Industry Applications, the IEEE Industrial Electronics, and the IEEE Circuit and System Societies. He was the recipient of the 2008 Young Author's Award for Practical Application from the Society of Instrument and Control Engineers (SICE), Japan. He received the Best Paper Award at the 2013 IEEE International Conference on Power Electronics and Drive Systems, the Best Paper Award of three papers from TaiPEA, during 2007–2010, one Excellent Paper Award at the National Symposium on Taiwan Electrical Power Engineering, 2009, two Excellent Paper Awards at the annual conference of SAE-Taipei, 2016 and 2017, the Dr. Shechtman Youth Researcher Award by the Taipei Tech, in 2018, the Outstanding Youth Electrical Engineer Award by the Chinese Institute of Electrical Engineering, the Special Outstanding Talent Award by the Ministry of Science and Technology, the Outstanding Education Achievement Award by the SAE-Taipei, the Outstanding Youth Control Engineer Award by the Chinese Automatic Control Society, in 2019, and the Outstanding Youth Engineer Award by the Chinese Institute of Engineers–Taichung Chapter, in 2020. He was named as an Outstanding Researcher by the College of Mechanical and Electrical Engineering, Taipei Tech in 2017 and 2018. Since 2017, he has been an Editor of the IEEE Transactions on Vehicular Technology.